

Wear Mechanisms of Carbon-Based Refractory Materials in SiMn Tap-Holes—Part II: *In Situ* Observation of Chemical Reactions

J.D. STEENKAMP, P. CHRIS PISTORIUS, and M. TANGSTAD

The purpose of the study presented here is to determine to what extent chemical reactions between carbon-based refractory and slag or metal in the tap-hole of a SiMn furnace can contribute to wear of tap-hole refractory. The results of the study are reported in two parts. In Part I, thermodynamic calculations suggested that reaction between silicomanganese slag and carbon-based tap-hole refractory is possible, and experiments with nominally pure materials support this. However, practical refractory materials are by no means pure materials and contain secondary phases and porosity which can be expected to affect reaction with slag. In Part II, such reactions are examined experimentally, in cup and wettability tests, using commercially available carbon block and cold-ramming paste refractory materials and mainly industrial SiMn slag. Clear evidence was found of chemical reaction at approximately 1870 K (approximately 1600 °C), forming SiC and, it appears, metal droplets. Both carbon block and ramming paste refractory reacted with slag, with preferential attack on and penetration into the binder phase rather than aggregate particles. The two types of carbon-based refractory materials showed similar extents of chemical reaction observed as wetting and penetration in the laboratory tests. The differences in refractory life observed practically in industrial furnaces should therefore be attributed to wear mechanisms other than pure chemical wear as studied in this work.

I. INTRODUCTION

THIS work examined whether chemical reaction between carbon-based refractory and slag in the tap-hole of a SiMn furnace could contribute to refractory wear.

As shown in Part I, reaction between silicomanganese slag and carbon-based refractory is expected, forming SiC as product and possibly also Si-Mn metal for temperatures above approximately 1850 K (approximately 1580 °C). The reactions are summarized in Table I.

In this paper, reaction between slag and industrial refractory materials was tested in two ways: by examining the slag–refractory interface after exposure to elevated temperature and by observation *in situ* in a wettability test. Wetting of carbon refractory by slag can be used to indicate the occurrence of reaction because slag should not wet the carbon refractory if no reaction

was to occur; however, if the slag was to react with the refractory, wetting would be expected.^[1]

The expected non-wetting behavior in the absence of chemical reaction between slag and refractory was confirmed experimentally, as shown later (Figure 2(a)). Non-wetting is also predicted by applying the Cassie expression,^[2] according to which the cosine of the effective contact angle between a liquid droplet and a heterogeneous substrate is the weighed average of the cosines of the contact angles between the liquid and each of the surface types (Eq. [1]).

$$\cos \theta_{\text{eff}} = \sum X_i \cos \theta_i. \quad [1]$$

In Eq. [1], X_i is the area fraction of surface i , and θ_i is the contact angle between the liquid and surface i . Based on the literature values of contact angles between slag and the main phases in carbon block, the average contact angle is predicted to be 95 deg (non-wetting) in the absence of reaction (Table II).

II. EXPERIMENTAL METHOD

The slag and refractory materials used in the experiments were described in Part I. Industrial refractory materials were used, with industrial slag used in most tests.

The industrial slag not only consisted primarily of an amorphous slag phase but also contained moissanite (SiC), alabandite (MnS), and intermetallic phases in

J.D. STEENKAMP, formerly Graduate Student with the Department of Materials Science and Metallurgical Engineering, University of Pretoria, South Africa, is now Chief Engineer with the Pyrometallurgy Division, Mintek, Randburg, South Africa. P. CHRIS PISTORIUS, POSCO Professor, is with the Department of Materials Science and Engineering, Carnegie Mellon University, Pittsburgh, PA, and also Extraordinary Professor, with the Department of Materials Science and Metallurgical Engineering, University of Pretoria. Contact e-mail: pistorius@cmu.edu M. TANGSTAD, Professor, is with the Department of Materials Science and Engineering, Norwegian University of Science and Technology (NTNU), Trondheim, Norway.

Manuscript submitted November 17, 2014.

Article published online December 24, 2014.

Table I. Potential Reactions Responsible for Wear of Carbon-Based Refractory by Slag in the Tap-Hole of a SiMn Furnace

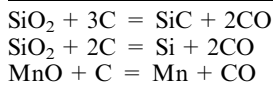


Table II. Input Values for Estimating Effective Contact Angle (θ_{eff}) of Slag on Carbon Block: Wettability Data for Slags on Relevant Solid Substrates Taken from the Literature, and Volume Fractions (X_i) of Phases in Carbon Block Estimated from Composition Reported in Part I

Surface i	X_i	θ_i (deg)	Reference
Graphite	0.8	110	Fig. 8 in Ref. [3]
SiC	0.1	20	Fig. 8 in Ref. [4]
Corundum	0.1	10	Fig. 6 in Ref. [3]

metal droplets (SiMn , Mn_5Si_3 , and Mn_7C_3). The bulk chemical analysis of the as-received slag was 8 pct MnO, 45 pct SiO_2 , 23 pct CaO, 7 pct MgO, and 17 pct Al_2O_3 by mass as determined by wet chemistry methods.

In both carbon block and cold-ramming paste refractory material, carbon was present both as large aggregate particles and in the matrix or binder phase. The carbon block had moissanite (SiC), and corundum (Al_2O_3) added intentionally to the binder phase.

A. Cup Tests

Static cup testing was used, as commonly applied in studies on slag/refractory interaction.^[5] To prepare the cups, samples of carbon block were machined into crucibles with OD (outer diameter) 65 mm, ID (inner diameter) 25 mm, EH (external height) 70 mm, and IH (internal height) 45 mm—see Figure 1. As shown in Figure 1, cold-ramming paste crucibles were prepared using an outer shell machined from graphite with OD = 65 mm, ID = 55 mm, EH = 70 mm, and IH = 60 mm. Ramming paste was rammed by hand around a spacer creating a cavity with ID = 25 mm and IH = 45 mm. Rammed crucibles were placed in steel cans on a layer of carbon powder, covered with refractory paper and carbon powder, heated in a muffle furnace to 1223 K (950 °C) at a rate of 40 °C/h, and baked for 30 minutes. The furnace was subsequently switched off and cooled overnight to room temperature.

For each cup test, a crucible with its cavity filled to the top with crushed slag (40 to 45 g) was placed in a high-frequency induction furnace. The experiments were conducted in argon which was purified by flowing the argon through a column containing zirconium turnings at 573 K (300 °C). Once the furnace was sealed, the chamber was flushed with argon at a flow rate of 1.8 dm³/min for 40 minutes. Once the temperature ramp started, the argon flow rate was reduced to 0.7 dm³/min. The chamber volume was 0.074 m³. The temperature was changed as follows: heating to 1673 K, 1773 K, or 1873 K (1400 °C, 1500 °C, or 1600 °C) in 1 hour,

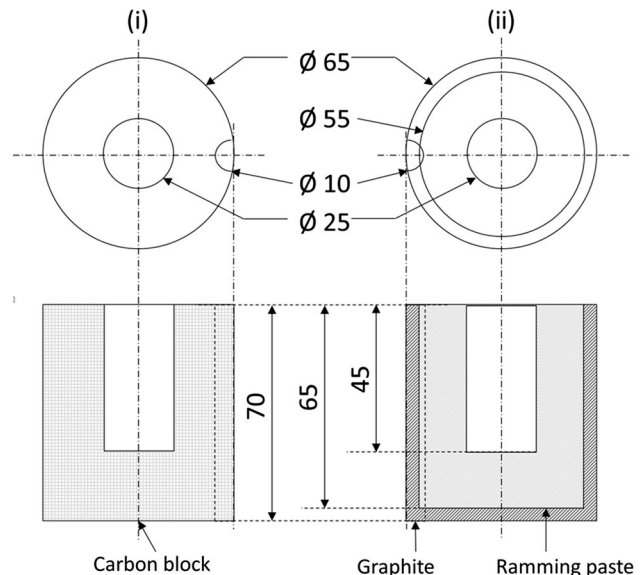


Fig. 1—Design of crucibles utilized in cup tests, showing (i) crucible machined from carbon block and (ii) ramming paste crucible with graphite shell. All dimensions in millimeters.

holding at temperature for 4 hours, switching off power, and opening up furnace to cool overnight to room temperature.

Cooled samples were removed from the furnace, and the crucibles filled with epoxy resin to keep the contents in position. Once the resin cured, the samples were cut in half and polished. After testing in contact with slag, no significant change in the internal diameter of any of the samples could be determined by visual inspection or measurement using the caliper method applied by Mølne⁶s.^[6] Instead, chemical wear and infiltration were studied at microscopic level by examining polished sections by optical microscopy and scanning electron microscopy with energy-dispersive X-ray microanalysis (SEM/EDS).

B. Wettability Tests

The experimental configuration for the wettability tests was described before.^[7] In these experiments small initially cylindrical slag samples were heated on a flat refractory substrate while observing the sample shape with a digital video camera. To form the cylinders, slag was ground to particles smaller than 106 μm and then compressed into a pellet with volume approximately 0.013 cm³. Heating was by means of a graphite element which was exposed to the furnace atmosphere. In these experiments, the gas atmospheres were at 1 atm total pressure. Either CO-gas or argon gas was supplied at gas flow rate of 0.50 dm³/min. The 99.9999 pct Ar gas was purified to remove moisture, oxygen, and hydrocarbons and subsequently passed over Mg turnings at a temperature of 673 K (400 °C) prior to entering the furnace. The CO-gas atmosphere would be more representative of actual industrial conditions; the argon gas atmosphere was used both as reference and to study the

Table III. Experimental Conditions of Wettability Tests

	Slag	Refractories	Temperature [K (°C)]	Atmosphere	Time (min)
1	synthetic	ramming paste matrix	1861 (1588)	argon	25
2	industrial	carbon block	1861 (1588)	argon	25
3	industrial	ramming paste matrix	1861 (1588)	argon	25
4	industrial	ramming paste aggregate	1861 (1588)	argon	25
5	industrial	ramming paste matrix	1861 (1588)	CO	25
6	industrial	ramming paste aggregate	1861 (1588)	CO	25
7	industrial	carbon block	1861 (1588)	CO	25

potential for chemical reaction between slag and refractory.

Temperature was measured using both a two-color pyrometer focused on the edge of the graphite sample holder, and a type C thermocouple installed inside the furnace just above the sample. The pyrometer reported reliable results at temperatures above 1173 K (900 °C). Temperature measurements were validated by observing melting as ball formation of pure iron on a pure alumina substrate in argon while heating at 5 °C/h.

The experimental conditions are summarized in Table III, and the wettability experiments are illustrated in Figure 2.

After experiments, vertical cross sections through the slag and refractory were prepared, similar to the method described by Ciftja *et al.*^[7]. The samples were mounted in resin and subsequently cut in half through the center of the substrate and slag droplet, grinding the section with SiC paper and polishing with diamond paste, cleaning with soap and water, and ethanol, and finally drying with hot air. The polished sections were examined by reflected-light optical microscopy and scanning electron microscopy.

As illustrated in Figure 2(a), melting of the slag could be inferred from a change in shape from the original cylindrical pellet, to a non-wetting droplet. Visible melting generally occurred close to approximately 1470 K (approximately 1200 °C), just below the slag liquidus temperature indicated as the balling temperatures shown in Figure 2(c). The calculated liquid fraction at the balling temperatures was around 90 pct. Wetting, indicative of reaction between the slag droplet and the refractory, occurred upon heating to much higher temperatures, generally higher than approximately 1770 K (approximately 1500 °C) as seen in Figure 2(b).

In addition to slag droplet shape changes due to increased wetting, the visible volume of the droplet also changed. The numerical values labeled in Figure 2(d) give the relative visible volume. The contact angle and volume were measured and estimated as follows:

For each experiment, wetting angles were measured on video images at 30-second intervals from the time at which the slag melted as indicated by “balling” until the time at which the holding temperature was reached, and subsequently at 5-minute intervals while the sample remained at the holding temperature. The results were based on three measurements taken 10 seconds apart after each 5-minute interval. In most instances, the contact angle measured at the two ends of the droplet

image differed, especially in cases where a second phase or droplet formed that appeared to prevent the liquid from moving freely. Contact angles from cases where such interference was apparent were not included in subsequent analysis.

To determine the random variation in the wetting angle measurements, two sets of images were prepared from the experiment where synthetic slag was melted on a ramming paste matrix substrate in an argon atmosphere. One set of images was for non-wetting conditions defined as from the onset of “balling.” The other set of images was for wetting conditions, *i.e.*, from the end of the experiment during the cooling down period. Each set consisted of thirty images of which 20 were a time series taken at 1-second intervals, and 10 were repeats of a single image, 5 were the image as taken, and 5 were the same image flipped horizontally. Image numbers were randomized before measurements. The results in Table IV show that the variability of the measured angles between repeats, and between the two positions in the droplet image, left and right, is generally less than the standard deviation of the measured angles.

To test the repeatability of the experimental conditions, the wetting angle measurements were compared from two experiments, each conducted in duplicate. Both pairs of experiments were for a holding temperature of 1861 K (1588 °C), under argon, using industrial slag. In one case, the substrate was ramming paste aggregate, and in the other, it was ramming paste binder matrix. The measured contact angles from the two pairs of experiments are compared in Figure 3(b); in each case, contact angles measured at the same duration after reaching the holding temperature are compared. In most cases, the differences are less than ±4 deg, the range bounded by the broken lines in the figure.

To quantify the change in droplet size, the assumption was made that the liquid droplet above the refractory substrate could be represented by a spherical cap,^[8] with the volume given by Eq. [2]^[9]; see Figure 3(a) for the definitions of the lengths a and h .

$$V_{\text{cap}} = 1/6\pi h(3a^2 + h^2). \quad [2]$$

Because no calibrated length scale was available for the video images, the volume of the slag upon “balling” was selected as reference volume (V_{ref}) and all other measurements expressed relative to this volume (V_x/V_{ref}).

Repeatability of volume measurements was tested using the same images used in testing the repeatability of

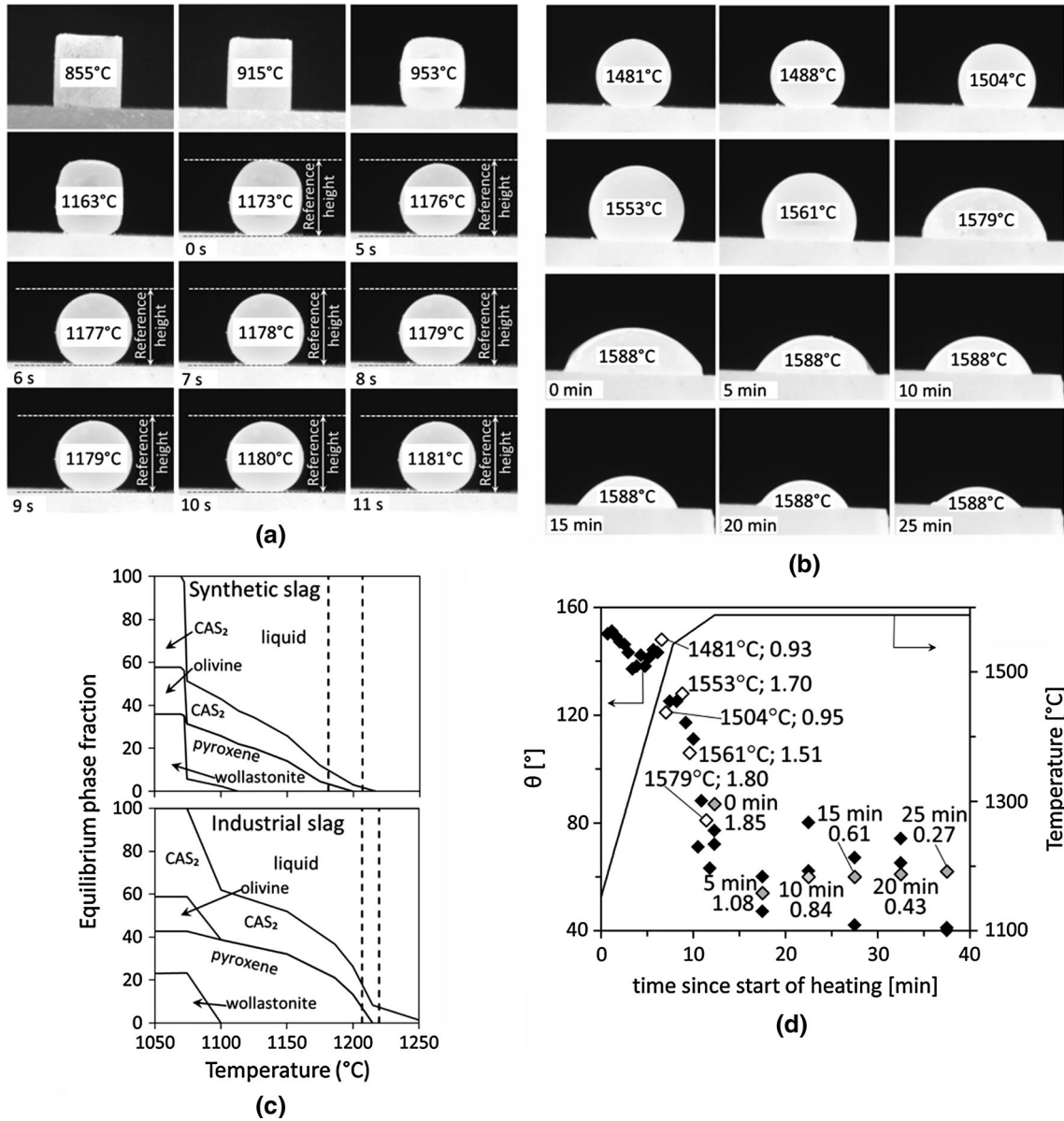


Fig. 2—Main features of wettability tests (synthetic slag on ramming paste matrix under argon), showing in (a) and (b) video images of slag droplet, during (a) initial melting (non-wetting) and (b) reaction (wetting). (c) Calculated phase equilibria (solid lines) compared with observed range of balling temperatures (vertical broken lines). (d) Sample temperature (solid line) and measured contact angles (data points). Labeled points correspond to the images in (b); dimensionless values give slag volume relative to the volume upon balling.

Table IV. Repeatability of Wetting Angle Measurements, in Degrees, on Left-Hand (θ_L) and Right-Hand Sides (θ_R) of Droplet, for a Time Series of 20 Consecutive Images and 10 Repeats of a Single Image, for Both Wetting and Non-wetting Conditions

	Wetting				Non-wetting			
	Time Series		Repeat		Time Series		Repeat	
	θ_L	θ_R	θ_L	θ_R	θ_L	θ_R	θ_L	θ_R
Average	36.8	34.2	35.4	33.5	144.6	145.2	145.5	145.8
STDev	4.2	2.2	2.7	2.7	1.6	2.2	2.0	1.8

The dataset was taken from the experiment conducted with synthetic slag on ramming paste matrix substrate in an argon atmosphere. The holding temperature was 1861 K (1588 °C).

Table V. Comparison of Volume Ratio Measured from 20 Consecutive Images and from 10 Repeats of a Single Image Taken Under Wetting and Non-wetting Conditions for Experimental Conditions as for Table IV

	Wetting		Non-wetting	
	Consecutive	Single	Consecutive	Single
Average	1.01	1.04	1.01	1.01
STDev	0.03	0.04	0.01	0.02

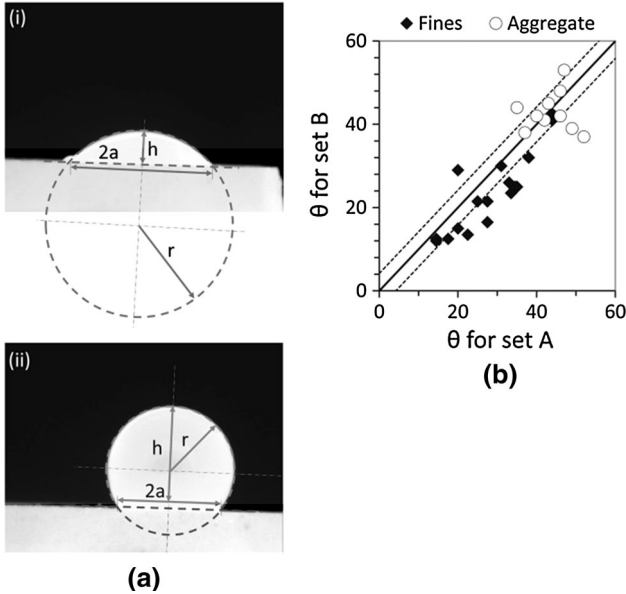


Fig. 3—(a) Definitions of parameters used in volume calculations of droplets, showing (i) wetting and (ii) non-wetting conditions. (b) Results of a reproducibility test: comparison of contact angles [industrial slag on ramming paste matrix and ramming paste aggregate; 1865 K (1592 °C); argon] measured at corresponding times in two runs for each substrate type. Most measurements are reproducible within ± 4 deg (indicated by broken lines).

contact-angle measurements. The results in Table V show that the average volume from 20 consecutive images and from 10 repeats of a single image differed by only a few percent.

III. RESULTS AND DISCUSSION

A. Wetting, Penetration, and Chemical Reaction

As shown in Figures 2(a) and (d), in the wettability tests under argon, the slag did not wet the refractory substrate at lower temperatures; wetting developed above approximately 1820 K (approximately 1550 °C). The development of wetting indicates chemical reaction between the slag and the refractory substrate. Similar observations were made in the much larger cup tests (Figure 4): In samples tested at the two lower temperatures, 1673 K and 1773 K (1400 °C and 1500 °C), the slag did not wet the refractory. However, the slag clearly

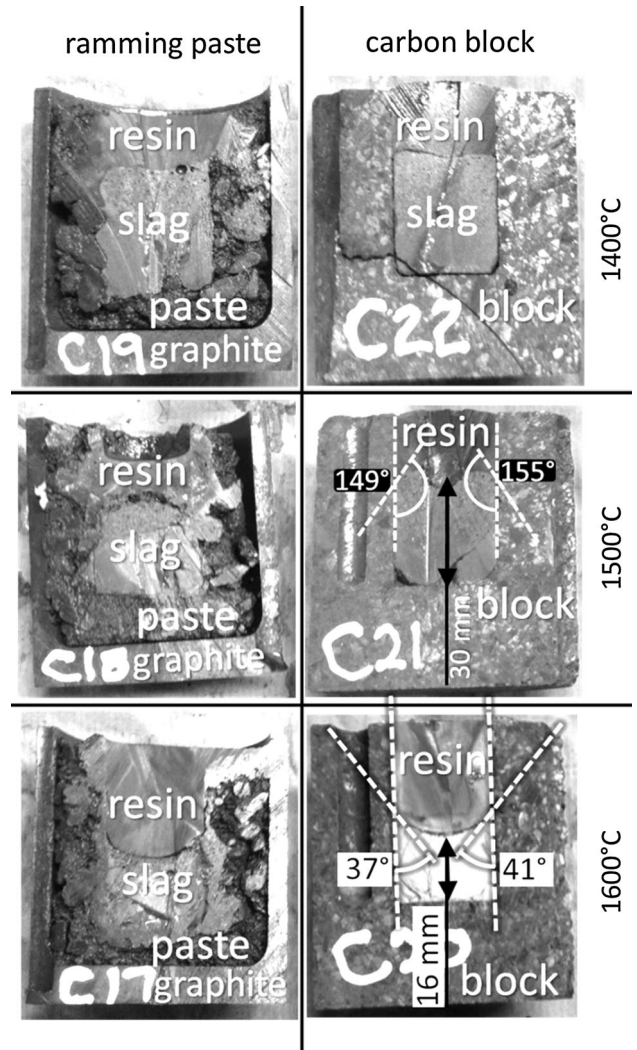


Fig. 4—Sectioned crucibles after cup tests, for (left) ramming paste and (right) carbon block exposed to industrial slag for 4 h, at different temperatures as indicated. Measured contact angles are shown in two cases.

Table VI. Cup Tests: Maximum Depth of Infiltration (mm) of Industrial Slag into Refractory After Testing to Different Maximum Temperatures

Temperature [K (°C)]	Carbon Block	Ramming Paste
1873 (1600)	4.0	3.7
1773 (1500)	0.5	0.8
1673 (1400)	0	0

Penetration measured by reflected-light optical microscopy on polished sections.

wetted cups made of carbon block and of ramming paste, after testing to 1873 K (1600 °C).

Similarly, little or no penetration of the slag into the refractory crucibles was observed in the lower-temperature cup tests, whereas substantial penetration was observed after testing to 1873 K (1600 °C); see Table VI.

Penetration into the refractory was also observed after the wettability tests (Table VII). The maximum depth of infiltration at each temperature was similar for the two refractory materials in the cup test (Table VI), but in the wettability test, the maximum depth of infiltration of slag into the carbon block was 2.7 times that of the ramming

Table VII. Wettability Tests: Maximum Depth of Infiltration of Industrial Slag into Refractory Samples After Holding at 1865 K (1592 °C), Under Argon; Measured in Images Shown in Fig. 6

Solid Phase	Infiltration Depth (mm)
Carbon block	2.7
Ramming paste aggregate	0.4
Ramming paste matrix	1.0

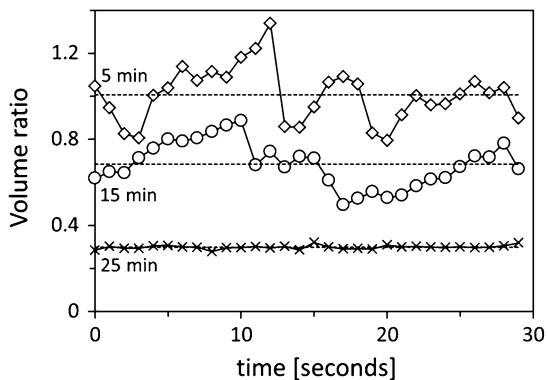


Fig. 6—Relative volume of synthetic slag on ramming paste matrix substrate [argon atmosphere; 1861 K (1588 °C)], for 30-s periods starting 5, 15, and 25 min into the holding period. Broken lines give the average relative volume for each 30-s time period.

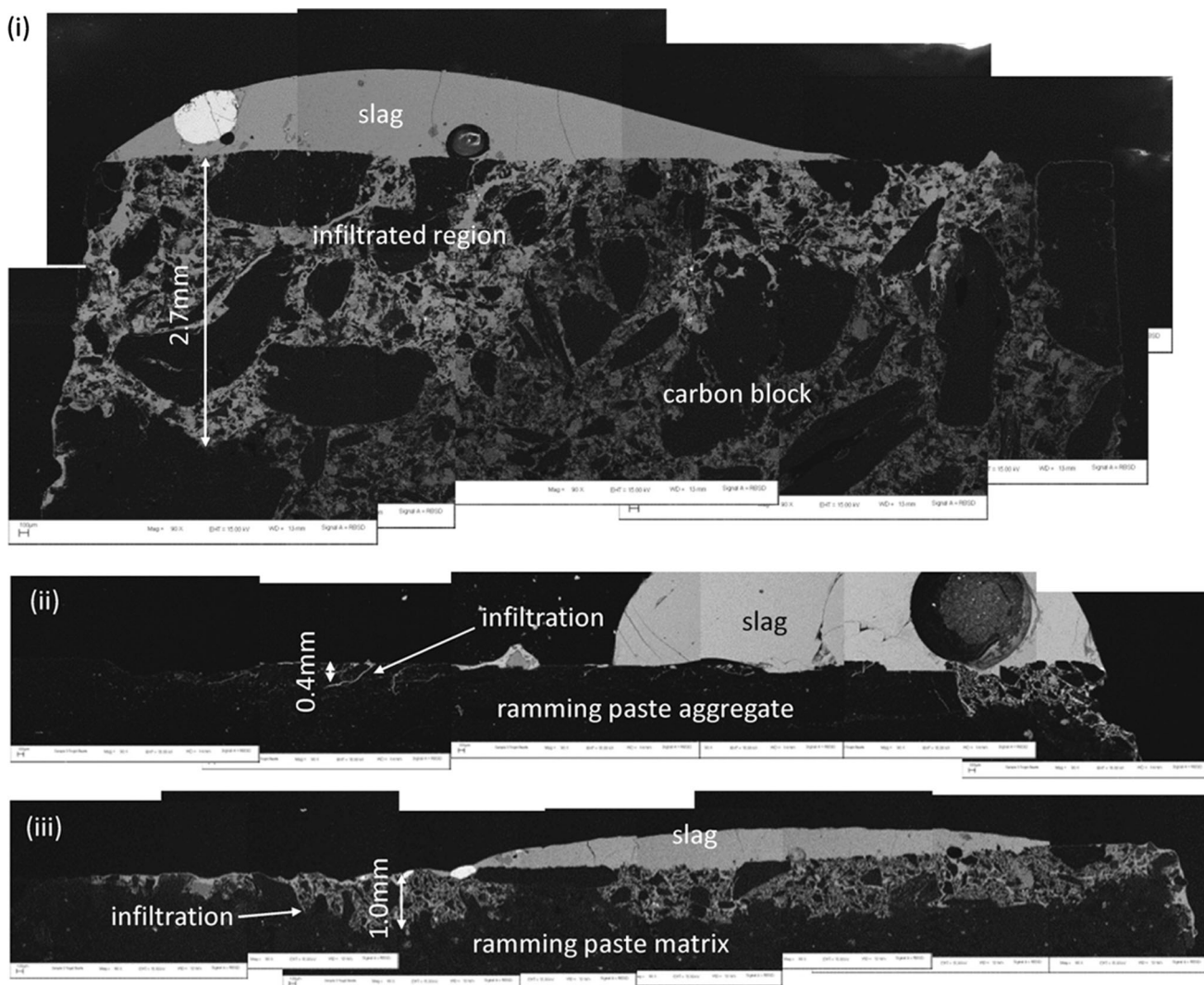


Fig. 5—Backscattered electron images of cross sections through samples after wettability tests [industrial slag; 1865 K (1592 °C); argon atmosphere]. Measurements in millimeter show depth of slag penetration into refractory.

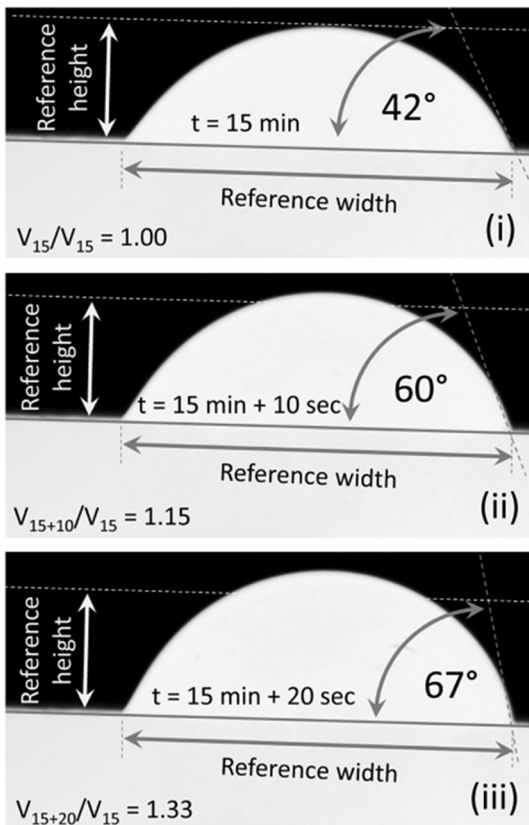


Fig. 7—Illustration of measured contact angle and slag volume, showing increase in volume presumably caused by gas formation. Images taken 10 s apart, starting 15 min into the holding period [synthetic slag on ramming paste matrix substrate under argon atmosphere; 1861 K (1588 °C)].

paste (Table VII; measured on polished sections—images shown in Figure 5). These differences in penetration for the different tests probably result from large differences in slag volume with less slag used in the wettability tests than in the cup tests. In all cases, penetration mainly occurred into the matrix (binder) component, rather than aggregate as seen in Figure 5. Changes in the volume of the visible slag droplet during the wettability test also confirmed slag penetration. As shown by the labels next to the data points in Figure 2(d), the visible slag volume decreased to 0.27 times the initial slag volume, at the end of the holding time—most of the slag had penetrated into the refractory.

In contrast, increases in slag volume were observed earlier in the holding period—as shown in Figure 2(d). At times, the slag droplet had a calculated volume up to 1.85 as large as the initial volume upon melting. Volume increases coincided with the rapid decrease in wetting angle; the volume likely increased because of formation of gaseous reaction products. The most likely gaseous reaction product as discussed in Part I is CO, formed by the reaction of SiO₂ in the slag with C in the refractory material to form CO and SiC. Examining the video recordings at higher time resolution showed that the slag volume fluctuated early in the holding period (Figure 6)—consistent with formation of CO bubbles at the slag–refractory interface, temporary hold-up of the gas bubbles in the slag droplet, followed by coalescence and escape of the bubbles. The smaller visible slag volume after the 25 minutes of holding (Figure 6) is qualitatively consistent with the subsequently observed penetration of slag into the refractory material (Figure 5). The average relative volume ratio was 1.01 at 5 minutes, 0.68 at 15 minutes, and 0.30 at 25 minutes. The range of

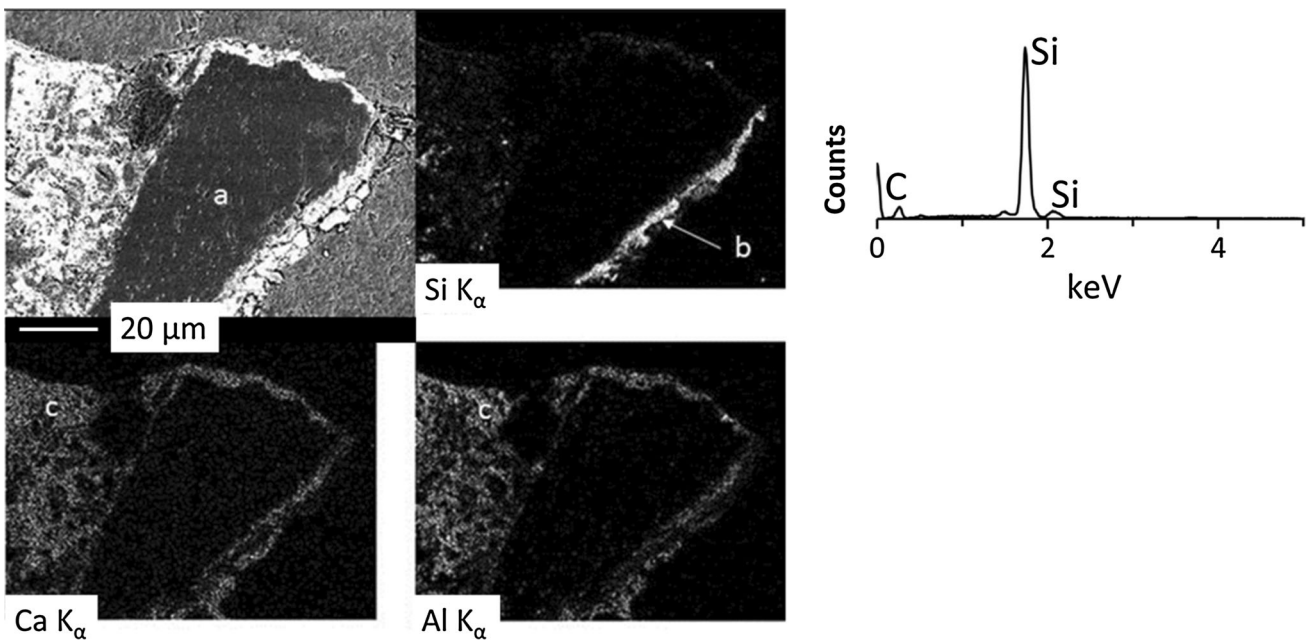


Fig. 8—SiC reaction product (“b”; EDX spectrum at right) shown by EDS elemental maps and backscattered electron image (top left), after exposing ramming paste to synthetic slag [argon atmosphere; 1861 K (1588 °C)], showing (a) refractory aggregate, (b) SiC reaction product, and (c) refractory matrix infiltrated by slag. Images and spectrum measured at 15 kV acceleration voltage.

the volume ratio decreased during the holding period, with the range being 0.79 to 1.34 (range: 0.55) after 5 minutes, 0.50 to 0.89 (range: 0.39) after 15 minutes, and 0.28 to 0.32 (range: 0.04) after 25 minutes, perhaps indicating a decrease in gas bubble formation rate.

Figure 7 illustrates the difference in slag volume in three images taken 10 seconds apart, 15 minutes into the holding period. As shown in the images, the diameter of the base of the slag droplet remained constant, but the height of the spherical cap increased, reflecting evolution of gaseous product.

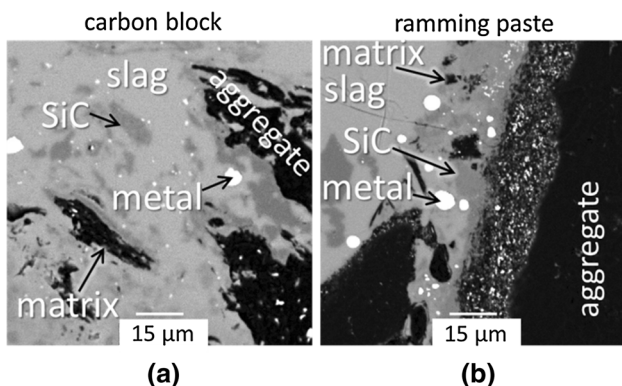


Fig. 9—Backscattered electron images of slag–refractory interface after cup tests [industrial slag; 1873 K (1600 °C); 4 h] with (a) carbon block and (b) ramming paste.

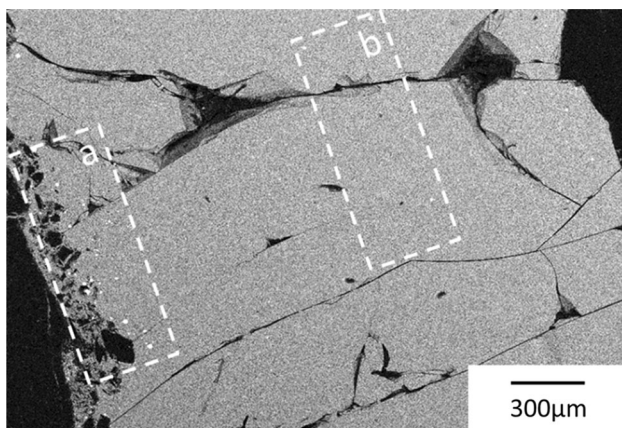


Fig. 10—Backscattered electron micrograph indicating the presence of small metal droplets (bright spots) concentrated near the ramming paste refractory (region “a”), with less metal in the bulk industrial slag away from the sidewall (region “b”). From cup test: ramming paste; industrial slag; 1873 K (1600 °C); 4 h.

B. Solid and Liquid Reaction Products

As discussed in Part I, the as-received industrial slag contained some silicon carbide and some metal droplets, creating ambiguity in identifying silicon carbide and metal as reaction products after the cup and wettability tests. However, as illustrated in Figure 8, the wettability test with synthetic slag showed unambiguous evidence of silicon carbide formation. The synthetic slag did not contain any silicon carbide before reaction, but silicon carbide was clearly present at the refractory–slag interface after the wettability test—confirming chemical reaction between slag and refractory, as predicted by thermodynamic calculations and inferred from the changes in wettability and slag volume.

For the cup tests, which used industrial slag, silicon carbide and metal were clearly present after the tests although identifying these as reaction products is inherently more ambiguous. Backscattered electron images of the carbon block and ramming paste exposed to industrial slag at 1873 K (1600 °C) in cup tests are presented in Figure 9. As discussed in Part I, the phases identified in the as-received carbon block were carbon-based aggregate, carbon matrix, SiC, and corundum. All of these phases remained to some extent after reaction, with the exception of corundum which dissolved in the slag. In addition, metal droplets were present after the cup tests, and silicon carbide was evident in the slag near the unreacted aggregate (Figure 9(a)).

Pre-fired ramming paste contained carbon aggregate, carbon matrix, SiC, quartz, cementite, and mullite as discussed in Part I. After reaction, the phases present were solidified slag, SiC, metal, carbon matrix, and carbon aggregate (Figure 9(b)); similar to the carbon block, oxides in the refractory dissolved in the slag.

The backscattered electron images of both carbon block (Figure 9(a)) and ramming paste (Figure 9(b)) after reaction indicate that the binder (matrix) phase reacted extensively with the slag, with less reaction by the particles of aggregate.

There were also indications that metal is formed by metal–slag reaction where such reaction would also have evolved CO: after the cup test at 1873 K (1600 °C), metal droplets were evident in the slag close to the ramming paste refractory on the sides and bottom of the crucible. The metal droplet concentration appeared to be much higher close to the crucible than in the bulk of the slag—see Figure 10 with quantification presented later. To test whether the metal droplets at the slag/refractory interface could have originated from the industrial slag or might have formed as reaction product, apparent metal droplets sizes were estimated from polished sections, and compositions were measured by microanalysis. Because of stereological effects,

Table VIII. Calculated Terminal Velocity (u_T) and Settling Distance After 4 h (Δz) for Different Metal Droplet Diameters (d_{droplet}) in Slag at 1873 K (1600 °C), Estimated with the Hadamard–Rybczynski Expression

d_{droplet}	μm	1.0	10.0	24.5	287.0	480.0
u_T	m/s	1.8E–09	1.8E–07	1.1E–06	1.5E–04	4.3E–04
Δz	mm	0.027	2.7	16.0	2193	6135

the droplet diameters on two-dimensional sections are on average smaller than the true droplet size, but measured diameters were used to obtain a first estimate of sizes; diameters were measured using ImageJ.^[10]

Size affects droplet settling rate, and droplet composition is important because the Si:Mn ratio of metal formed by slag-refractory reaction is expected to be different from that of the bulk ferroalloy. For the metal compositions listed in Part I, the molar ratio Si:Mn in

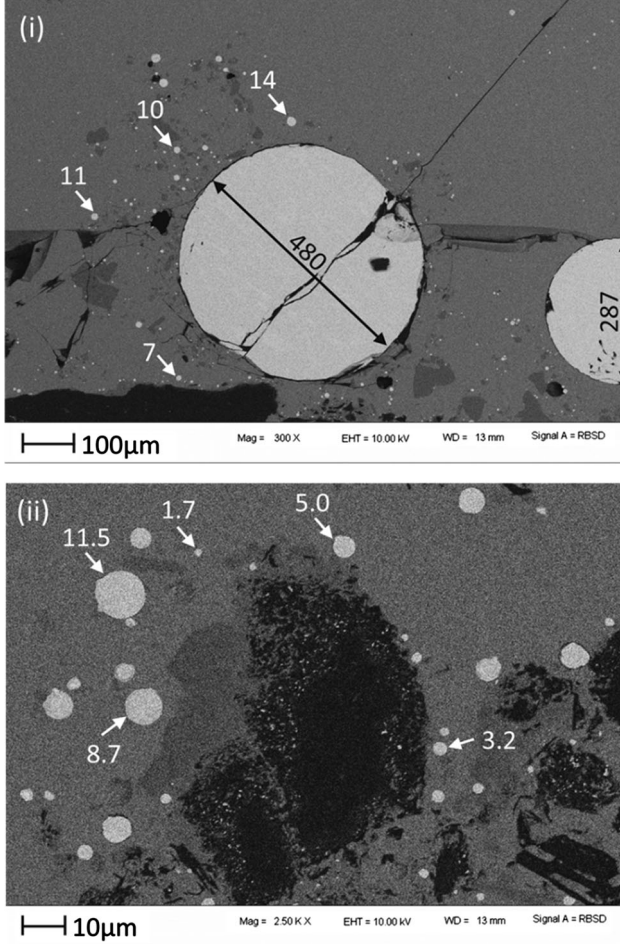


Fig. 11—Backscattered electron images showing metal droplets (bright areas labeled with measured diameters in μm) in slag close to refractory, after cup test at 1873 K (1600 °C) for 4 h (ramming paste crucible; industrial slag).

the bulk metal would be approximately 0.58 based on published metal compositions, but 0.44 in metal formed by reaction of silicomanganese slag with graphite at 1873 K (1600 °C). Therefore, the Si:Mn molar ratio is expected to be lower in metal droplets formed by slag-refractory reaction than in entrained metal in the tapped slag.

Possible settling distances of metal droplets in the slag during the test lasting 4 hours at 1873 K (1600 °C) were estimated with the Hadamard–Rybczynski expression (Eq. [3]).^[11]

$$u_T = \frac{gr^2(\rho_{\text{metal}} - \rho_{\text{slag}})}{3\mu_{\text{slag}}}. \quad [3]$$

In Eq. [3], u_T is the terminal velocity, g gravitational acceleration, r the droplet radius, ρ_i the density of phase i , and μ_{slag} the slag viscosity. Specific values used in this calculation were $\rho_{\text{metal}} = 4.4 \times 10^3 \text{ kg/m}^3$ as estimated from the metal composition using a rule of mixtures,^[12] $\rho_{\text{slag}} = 2.8 \times 10^3 \text{ kg/m}^3$, and $\mu_{\text{slag}} = 0.74 \text{ kg/ms}$ based on published correlations.^[13] Calculated terminal

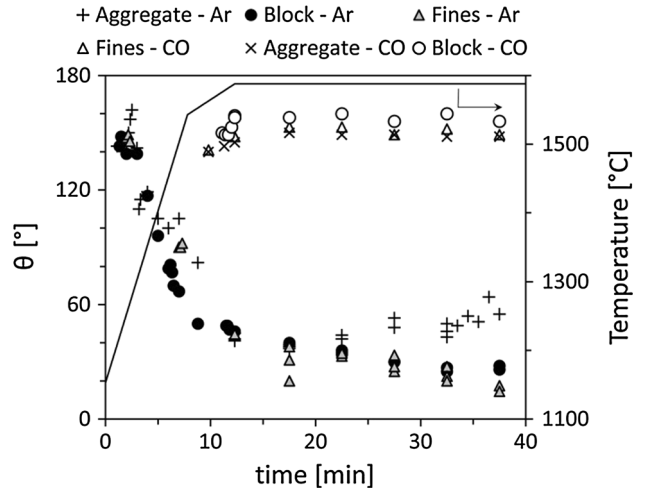


Fig. 12—Comparison of contact angles (data points) for industrial slag on different substrates (carbon block, ramming paste aggregate, and ramming paste matrix), under argon (filled symbols; wetting develops) and CO (open symbols; non-wetting throughout the measurement); holding temperature 1861 K (1588 °C).

Table IX. Composition of Metal Droplets (Mass Percentages; Carbon not Analyzed) in Industrial Slag After Reaction with Ramming Paste at 1873 K (1600 °C) for 4 h

Category	Average				Standard Deviation			Si:Mn Molar Ratio (Average, with 95 pct Confidence Limits)
	pctSi	pctMn	pctFe	pctTotal	pctSi	pctMn	pctFe	
a Large	21.8	71.8	6.4	100.0	—	—	—	0.59
b Large	14.7	76.6	8.7	100.0	—	—	—	0.38
c 5 to 10 μm in slag	19.4	76.6	4.0	100.0	4.4	6.7	2.7	0.51 ± 0.29
d 5 to 10 μm at interface between slag and reaction zone	17.3	79.2	3.5	100.0	5.9	8.3	3.0	0.44 ± 0.38

EDS analyses performed at 10 kV; average of ten droplets per category except for the two large droplets *a* and *b*.

velocities and settling distances—given by $\Delta z = u_T t$, for $t = 4$ hours are given in Table VIII. Evidently, only metal droplets with diameters larger than approximately $25 \mu\text{m}$ would have settled the full depth of the slag of 16 mm in these tests during 4 hours, to accumulate at slag/refractory interface at the bottom of the crucible.

Although droplets smaller than $10 \mu\text{m}$ would only have settled from a fraction of the slag depth, such small droplets were found both near the bottom of the crucible and near the crucible wall, indicating that the droplets are formed by chemical reaction; as shown in Figure 10, small droplets were much more prevalent close to the crucible wall than in the bulk of the slag. Image analysis conducted with ImageJ^[10] of the micro-graph in Figure 10 indicated that in area *a* which was close to the slag–refractory interface, the area fraction of bright metal droplets was 0.93 pct, significantly greater than in area *b* which was the bulk slag with the area fraction of metal 0.29 pct (Figure 11).

While the position of small metal droplets did suggest that the droplets are formed by chemical reaction, the results from microanalysis did not give a clear indication. Figure 9 shows some of the analyzed droplets for which results are summarized in Table IX. Because calcium is not present in the metal to a significant level, all analyses with more than 1 pctCa were taken to be affected by the surrounding slag and were not included in the averages. Given the variability in the compositions (Table IX), the analyses did not give any indication of the provenance of the metal droplets.

C. Non-wetting in CO Atmosphere

Several wettability tests were performed using CO as atmosphere instead of argon as seen in Table III. Measured contact angles are reported in Figure 12 with the results for argon included in the figure for comparison. Evidently, conditions remained non-wetting for the duration of the experiments in CO, for all three substrate types. In addition, the “balling temperature” which was based on visible slag melting and droplet formation was much higher in CO than in argon. In Figure 12, the balling temperature can be found as the temperature at the time for which the first contact angle is reported—in CO; this was around 1840 K (around 1570 °C) in all cases. For experiments conducted in CO, the balling temperature was much higher than the liquidus temperature of approximately 1490 K (approximately 1220 °C), whereas for experiments conducted under argon, the balling temperature was much lower and agreed with the liquidus temperature.

A further difference with the measurements under argon is that—as illustrated in Figure 13—slag penetration did not occur for experiments in CO. Figure 13 shows the relative slag volume, calculated from the observed slag droplet size. For experiments in CO, the relative volume remained close to 1. The average relative volume was 0.99 at 5 minutes, 1.06 at 15 minutes, and

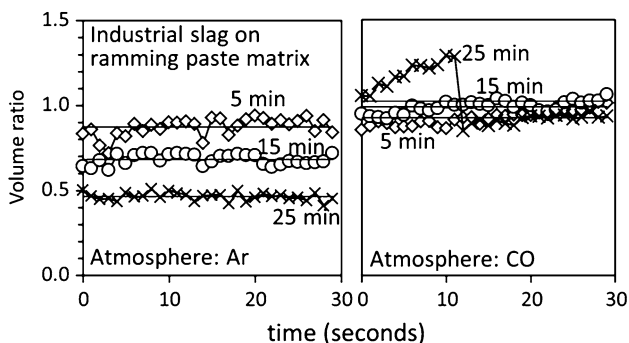


Fig. 13—Relative volume of industrial slag droplet on ramming paste matrix substrate under (left) argon (slag penetrates refractory), and (right) CO (slag does not penetrate); 1861 K (1588 °C). Relative volumes shown for 30-s periods starting at 5, 15, and 25 min into the holding period. Horizontal lines give the average relative volume ratio for each 30-s period.

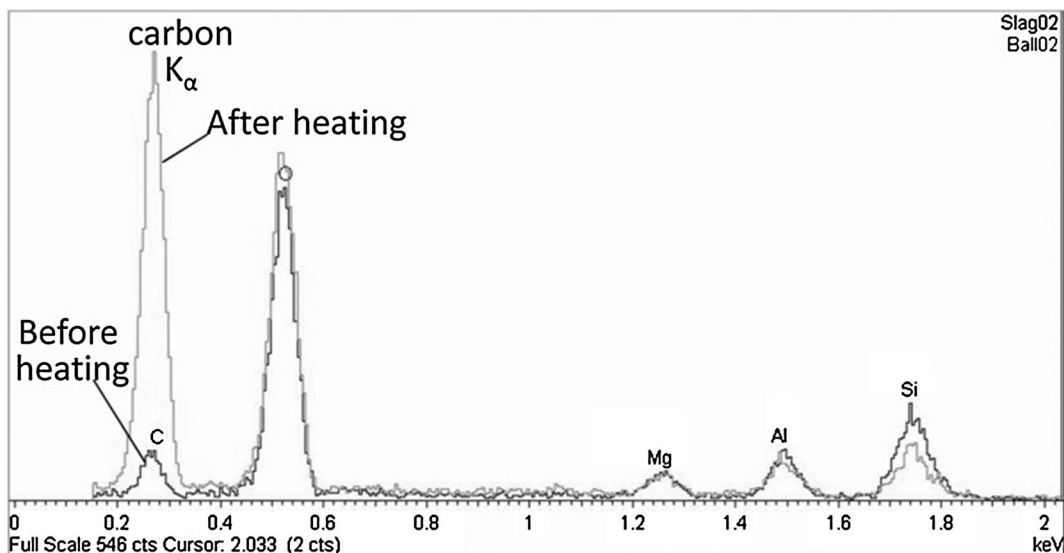


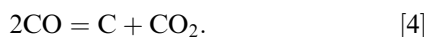
Fig. 14—EDS spectra (area analyses; 5 kV accelerating voltage) of powdered industrial slag before heating (“Slag02”) and industrial slag ball after wettability test in CO at 1861 K (1588 °C) (“Ball02”). Note the much larger carbon peak in the latter case.

1.09 at 25 minutes. However, the *range* of volume fluctuations was similar to the range in argon, and—at least for the run examined—remained approximately constant with time. The range was 0.91 to 1.09 (width of range 0.18) at 5 minutes and 0.98 to 1.13 (width of range 0.15) at 15 minutes. After 25 minutes, an apparent gas bubble collapse occurred during the 30-second-period study, increasing the range to 0.91 to 1.38 (width of range 0.47).

Since wetting of the refractory requires chemical reaction, it is concluded that significant slag–refractory reaction did not occur in the experiments performed in CO. However, the fluctuations in slag volume caused by gas evolution do indicate that chemical reaction did occur. The chemical reaction may have been between SiC and MnO in the slag or may have involved carbon deposited on the droplet surface by the CO atmosphere.

It does not appear possible that the presence of a CO atmosphere as such could have suppressed slag–carbon reaction, for the following reason. Under argon, gas evolution and substrate wetting were observed, and it seems reasonable to assume that the gas that formed was CO. This means that reaction between slag and carbon could nucleate CO bubbles at the reaction temperature; nucleation would have required a CO pressure slightly above the ambient pressure of 1 atm. During growth of such a bubble, the atmosphere at the reaction interface would have been essentially 1 atm CO, no different from the atmosphere supplied externally in experiments performed under CO. Indeed, in both cases where experiments were performed under Ar and under CO, volume fluctuations indicating gas evolution occurred. It hence appears that maintaining a CO atmosphere did not suppress slag–carbon reaction but rather changed the site of the reaction—from the slag–substrate interface under Ar, to the slag–gas interface under CO. This suggestion is supported by the absence of infiltration and non-wetting behavior in experiments under CO, indicating an absence of reactive wetting of the substrate. It is also supported by observation of deposited carbon on the slag surface for experiments under CO as discussed below—demonstrating that the CO atmosphere was a source of elemental carbon which could have reacted with the slag.

It is suggested that carbon could have been deposited on the surface of the slag, by Reaction [4]. Factors which would have promoted carbon deposition are the presence of the graphite heating element and the presence in the slag of Fe and MnO, which are known to catalyze carbon deposition.^[14,15] The element would have been hotter than the sample and hence an effective getter of any CO₂ in the incoming gas or product gas for Reaction. [4] The observed delay in slag agglomeration or balling could have been caused by deposited carbon: in mold fluxes used for continuous casting of steel carbon is added intentionally to control the melting rate by hindering slag agglomeration.^[16,17]



In further support of the suggested role of deposited carbon, EDS microanalysis (SEM, 5 kV) of an industrial slag ball—formed on carbon block substrate during a

wettability experiment conducted in CO—showed the presence of much more carbon than on the surface of milled industrial slag not exposed to a CO atmosphere; see Figure 14.

IV. CONCLUSIONS

As with the pure materials considered in Part I, industrial carbon-based refractory and industrial silico-manganese slag showed clear evidence of chemical reaction at approximately 1870 K (approximately 1600 °C), forming SiC and, it appears, metal droplets. Both carbon block and ramming paste refractory reacted with slag, with preferential attack on and penetration into the binder phase rather than aggregate particles.

The two types of carbon-based refractory materials investigated here showed similar extents of chemical reaction, defined in terms of wetting and penetration, in the laboratory tests. The differences in refractory life observed practically in industrial furnaces^[18] should therefore be attributed to wear mechanisms other than pure chemical wear as studied in this work.

ACKNOWLEDGMENTS

We are grateful to the anonymous industrial sponsor for providing guidance and funding the PhD Project of which the work presented formed part. We acknowledge the National Research Foundation of South Africa (Grant TP2011070800005) for leveraging the funding provided by the project sponsor.

REFERENCES

1. H. Sun, M.Y. Lone, S. Ganguly, and O. Ostrovski: *ISIJ Int.*, 2010, vol. 50, pp. 639–46.
2. A.B.D. Cassie: *Discuss. Faraday Soc.*, 1948, vol. 3, pp. 11–16.
3. P. Shen, H. Fujii, and K. Nogi: *Mater. Chem. Phys.*, 2009, vol. 114, pp. 681–86.
4. J. Safarian and M. Tangstad: *Metall. Mater. Trans. B*, 2009, vol. 40B, pp. 920–28.
5. S. Baxendale: in *Refractories Handbook*, C.A. Schacht, ed., CRC Press, Boca Raton, 2004, pp. 435–74.
6. H. Møltnås: MS Thesis, Norwegian University of Science and Technology, 2011.
7. A. Ciftja, T.A. Engh, and M. Tangstad: *Metall. Mater. Trans. A*, 2010, vol. 41A, pp. 3183–95.
8. N. Eustathopoulos, M.G. Nicholas, and B. Drevet: *Wettability at High Temperatures*, Pergamon Press, Amsterdam, 1999.
9. E.W. Weisstein: Spherical Cap, MathWorld—A Wolfram Web Resource. [Online]. <http://mathworld.wolfram.com/SphericalCap.html>. Accessed 11 Mar 2014.
10. W.S. Rasband: ImageJ, U. S. National Institutes of Health, Bethesda, Maryland. [Online]. <http://imagej.nih.gov/ij/>. Accessed 16 Jan 2014.
11. R. Clift, J.R. Grace, and M.E. Weber: *Bubbles, Drops and Particles*, Academic Press, New York, 1978, pp. 30–47.
12. J.D. Steenkamp: Ph.D. Thesis, University of Pretoria, 2014.
13. J. Muller and J.D. Steenkamp: *J. Manuf. Sci. Prod.*, 2013, vol. 13 (4), pp. 251–262.
14. D.H. Hubble: in *The Making, Shaping and Treating of Steel—Ironmaking Volume*, 11th ed., D.H. Wakelin, ed., The AISE Steel Foundation, Pittsburgh, 1999, pp. 161–228.

15. G.C. Allen and J.A. Jutson: *J. Mater. Chem.*, 1991, vol. 1 (1), pp. 73–78.
16. K.C. Mills, A.B. Fox, Z. Li, and R.P. Thackray: *Ironmak. Steelmak.*, 2005, vol. 32, pp. 26–34.
17. E. Wei, Y. Yang, C. Feng, I. Sommerville, and A. McLean: *Int. J. Iron Steel Res.*, 2006, vol. 13 (2), pp. 22–26.
18. Anonymous, Personal communication with plant personnel, 2010.